



Hydrodeoxygenation of lignin-derived phenolic compounds over bi-functional Ru/H-Beta under mild conditions



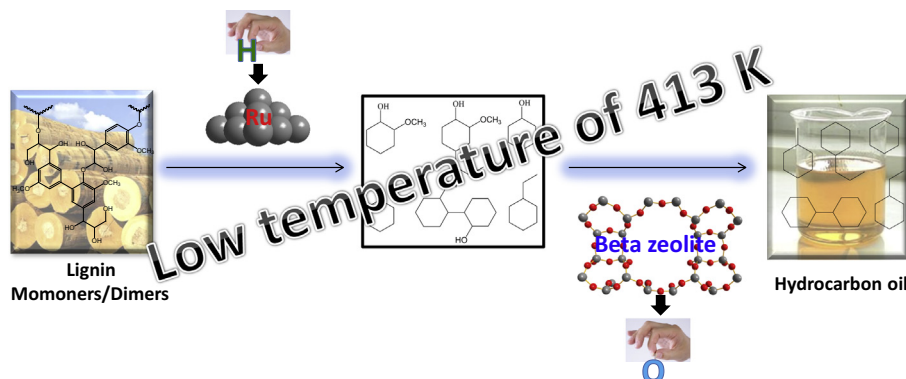
Gang Yao, Guangjun Wu*, Weili Dai, Naijia Guan, Landong Li*

Key Laboratory of Advanced Energy Materials Chemistry of Ministry of Education, Collaborative Innovation Center of Chemical Science and Engineering (Tianjin), Nankai University, Tianjin 300071, China

HIGHLIGHTS

- Remarkable performance in aqueous phase hydrodeoxygenation was achieved at 413 K.
- Bifunctional Ru/H-Beta was developed for lignin-derived compounds upgrading.
- Reaction conditions and catalyst constitution are crucial for the high activity.
- Hydrodeoxygenation reaction pathway on Ru/H-Beta was illustrated.

GRAPHICAL ABSTRACT



ARTICLE INFO

Article history:

Received 8 December 2014
 Received in revised form 7 February 2015
 Accepted 9 February 2015
 Available online 19 February 2015

Keywords:

Hydrodeoxygenation
 Lignin-derived phenolic compounds
 Bio-oil
 Ru/H-Beta catalyst

ABSTRACT

Bifunctional ruthenium catalysts supported on H-Beta zeolite were designed and applied in the hydrodeoxygenation of lignin-derived phenolic compounds for bio-oil upgrading. The oxygen-containing groups in lignin-derived phenolic monomers and dimers could be efficiently removed through aqueous phase hydrodeoxygenation catalyzed by Ru/H-Beta under very mild conditions, i.e. at 413 K and 4 MPa H₂. Characterization results revealed that ruthenium species existed in the form of highly dispersed nanoparticles on H-Beta zeolite, while the presence of both Brønsted and Lewis acid sites in zeolite was crucial for the remarkable hydrodeoxygenation activity. The effects of reaction conditions and catalyst constitution on the catalytic performance of Ru/H-Beta in hydrodeoxygenation were systematically investigated. The hydrodeoxygenation pathway of diphenyl ether as a model compound catalyzed by optimized 0.5%Ru/H-Beta was discussed and the structure-activity relationship in hydrodeoxygenation was proposed.

© 2015 Elsevier Ltd. All rights reserved.

1. Introduction

Nowadays, energy shortage and environmental pollution are two major problems all over the world. It is quite urgent to explore

new and renewable energy source with low NO_x and SO_x emissions. Lignocellulose has attracted great attention due to its abundant source, high energy content and low price [1,2]. After thermal processing, lignocellulose can be converted to bio-oil in the gasoline range with ~30 wt.% production of phenolic compounds, e.g. phenol, guaiacols and syringols. On the other hand, lignin cleavage under mild conditions is developed and phenolic monomers, e.g. phenol, alkyl-guaiacols, alkyl-syringols, and

* Corresponding authors. Tel./fax: +86 22 2350 0341.

E-mail addresses: wuguangjun@nankai.edu.cn (G. Wu), lild@nankai.edu.cn (L. Li).

dimers, e.g. β -O-4, 4-O-5 ether linkage and 5-5', β -1 C-C linkage, can be obtained [3–5]. However, the high oxygen content will reduce the quality of the phenolic bio-oils and a deoxygenation process is required to obtain alkane fuels with high energy content [6]. The upgrading of bio-oils through removing the excess oxygen atoms is most important and remains challenging.

Hydrodeoxygenation is an effective technology to remove the oxygen and convert lignin into high energy carriers such as cycloalkanes. Nickel [7–8], nickel sulfide [9], nickel phosphide [10] and nickel or cobalt in conjunction with molybdenum or tungsten [11–12] are employed as catalysts in hydrodeoxygenation processes. However, the intrinsic activity of these catalysts is rather low and high temperature is required for the hydrodeoxygenation upgrading process. Moreover, the product contamination by sulfur from sulfide catalysts is a serious problem to be considered. Noble metals with high aromatic hydrogenation activity are alternative choices of hydrodeoxygenation catalysts. Palladium [3,13–16], platinum [17–19], rhodium [20] and ruthenium [21–22] on different supports, e.g. active carbon, metal oxides and zeolites, have been evaluated in the hydrodeoxygenation process. For example, Kou et al. developed a two-step process for the degradation Birch wood and the hydrodeoxygenation of phenolic monomers and dimers into alkanes with Pd/C and H_3PO_4 at 473 K [3]. Brønsted acidic ionic liquids combined with nanoparticles were reported to be effective for hydrodeoxygenation by Yan et al. [23] and further investigated by Xu et al. [24]. It appears that remarkable hydrodeoxygenation efficiency can be achieved with the combination of Brønsted acids and active metals. However, the introduction of additional homogeneous Brønsted acids will probably cause the recycling and environmental problems. To address these issues, supported palladium nanoparticles and heterogeneous solid acids were proposed as combination catalyst system by Lercher et al. and remarkable activity in the hydrodeoxygenation of lignin-derived phenolic compounds could be achieved at 473 to 523 K [25]. Moreover, bi-functional catalysts composed of active metals on acidic supports, e.g. Pt/H-Y [26] and Ru/H-ZSM-5 [27], have been reported to be active for the hydrodeoxygenation process.

Despite current achievements on the hydrodeoxygenation of lignin-derived compounds, adequate catalysts working under mild conditions are still challenging. With a few exceptions [28–30], high reaction temperatures, e.g. >473 K, are required for the hydrodeoxygenation of lignin-derived phenolic dimers, making this process most energy-consuming and unfeasible for industrial application. In the present study, we will focus on the hydrodeoxygenation of lignin-derived phenolic mono- and dimers over bi-functional noble metals supported on acidic zeolite under mild conditions. The effects of catalyst constitution on hydrodeoxygenation activity are investigated and the hydrodeoxygenation reaction pathways are discussed.

2. Experimental methods

2.1. Preparation of catalysts

All the catalysts were prepared by impregnating the supports (H-Beta with Si/Al = 13.5, H-ZSM-5 with Si/Al = 12.5, H-USY with Si/Al = 12.5, H-MOR with Si/Al = 12.0, SiO_2 with surface area of $286.2 \text{ m}^2/\text{g}$ and $\gamma\text{-Al}_2\text{O}_3$ with surface area of $278.5 \text{ m}^2/\text{g}$) with aqueous solution of metal salts ($\text{H}_2\text{PtCl}_6 \cdot x\text{H}_2\text{O}$, PdCl_2 , $\text{RuCl}_3 \cdot x\text{H}_2\text{O}$ and $\text{RhCl}_3 \cdot x\text{H}_2\text{O}$). In a typical preparation process of Ru/H-Beta (1% Ru), 10 mL RuCl_3 aqueous solution was added to 1 g H-Beta support. The impregnated sample was well mixed and then evaporated in a rotary evaporator at constant temperature of 353 K. The as-prepared sample was carefully washed by distilled

water, dried at 353 K overnight and then reduced in 5% H_2 /He at 473 K for 2 h prior to being used as catalyst.

2.2. Characterization techniques

Specific surface areas and pore volumes were determined through N_2 adsorption/desorption isotherms at 77 K collected on a Quantachrome iQ-MP gas adsorption analyzer. XRD patterns were recorded on a Bruker D8 ADVANCE powder diffractometer using $\text{Cu K}\alpha$ radiation at a scanning rate of $4^\circ/\text{min}$. Metal loadings were analyzed by ICP-AES (Perkin Elmer Optima 2000). Solid samples were dissolved in hot aqua regia with the addition of several drops of HF and the excess acid in solution was removed by heating at constant temperature of 453 K before ICP analysis. TEM images were taken on a FEI Tecnai G2 F20 electron microscope at an acceleration voltage of 200 kV. Dispersion of noble metals was determined by CO pulse adsorption on a chemisorption analyzer (Chemisorb 2720, Micromeritics). Temperature-programmed desorption of ammonia (NH_3 -TPD) and temperature-programmed reduction by hydrogen (H_2 -TPR) were performed on a chemisorption analyzer (Quantachrome ChemBet 3000).

Fourier transform infrared (FTIR) spectra of pyridine adsorption were collected on the Bruker Tensor 27 spectrometer. A self-supporting pellet made of the sample was placed in the flow cell and evacuated under reduced pressure at 693 K for 4 h. After cooling to room temperature, the samples were saturated with pyridine vapor and then evacuated at 473 K for 30 min. Spectra were recorded at evacuation temperature in the $4000\text{--}650 \text{ cm}^{-1}$ range by using co-addition of 32 scans. The amount of the Lewis acid sites in samples was determined from the integral intensity of characteristic band at ca. 1450 cm^{-1} using the molar extinction coefficients of Emeis [31].

2.3. Catalytic evaluation and product analysis

The hydrodeoxygenation of various lignin-derived compounds (AR purity, from commercial suppliers and used as provided) was performed in a high-pressure stainless autoclave (15 mL in capacity) at a stirring rate of 800 rpm. After reaction, the autoclave was cooled down in ice water and the liquid products were collected and extracted with acetic ether for three times and then analyzed by gas chromatography (Shimadzu GC-2010) with a RXI-5MS column (30 m, 0.25 mm i.d., stationary phase thickness 0.25 μm). 2-isopropylphenol was used as an internal standard for quantification. The carbon balance was better than 90% in all cases.

3. Results and discussion

3.1. Physicochemical properties of samples

The physicochemical properties of supported catalysts are summarized in Table 1. The obtained metal loadings are very close to the designed values, indicating the high efficiency of impregnation process. High metal dispersion of $>50\%$ is obtained for all noble metals supported on zeolites, which should be good for catalytic applications due to the enhanced metal accessibility. Besides, the high surface areas ($450\text{--}700 \text{ m}^2/\text{g}$) and micropore volumes ($0.20\text{--}0.32 \text{ cm}^3/\text{g}$) of zeolite supports are well preserved. The pore diameter of supported Ru catalysts with similar metal loading of ca. 0.5% is observed to be Ru/H-USY (0.80 nm) $>$ Ru/H-Beta (0.78 nm) $>$ Ru/H-MOR (0.70 nm) $>$ Ru/H-ZSM-5 (0.49 nm). Large pore diameter is good for catalytic application especially when dealing with bulky reaction substrate, e.g. lignin-derived phenolic dimers.

Table 1
Physicochemical properties of samples under study.

Sample	Metal loading (%) ^a	Metal dispersion (%)	Si/Al ^b	S _{BET} (m ² /g)	Pore diameter (nm)
Pt/H-Beta	0.96	57.5	14.1	587	0.76
Pd/H-Beta	0.49	53.8	14.3	595	0.77
Rh/H-Beta	0.51	58.2	13.7	579	0.75
0.5%Ru/H-Beta	0.51	63.2	13.9	602	0.78
1%Ru/H-Beta	0.98	61.3	13.7	594	0.76
2%Ru/H-Beta	1.94	50.5	14.2	562	0.71
Ru/H-ZSM-5	0.51	52.6	12.9	542	0.49
Ru/H-MOR	0.52	55.8	13.2	476	0.70
Ru/H-USY	0.51	57.4	13.4	682	0.80
Ru/SiO ₂	0.51	39.7	/	275	/
Ru/Al ₂ O ₃	0.53	37.6	/	262	/

^a Determined by ICP.

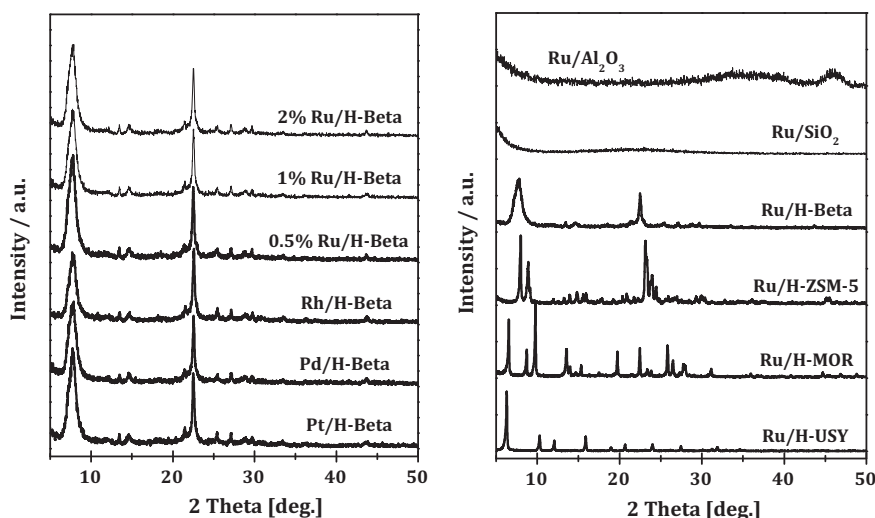


Fig. 1. XRD patterns of H-Beta supported catalysts and supported Ru catalysts.

For all samples, typical diffraction peaks corresponding to support materials are observed (Fig. 1), indicating the well preservation of support structure after the introduction of metal by impregnation. Besides, no diffraction peaks are observed for metals even after hydrogen reduction process due to the low metal loading and high dispersion, as confirmed in Table 1.

The TEM images of Ru/H-Beta samples with different Ru loadings are shown in Fig. 2, and it is seen that ruthenium species appear as small clusters (<4 nm) on the H-Beta supports. The cluster size distribution clearly reveals that the average size of ruthenium species increases slightly with increasing loading. Typically, smallest average cluster size of 1.6 nm is observed for 0.5%Ru/H-Beta, followed by 1.7 nm for 1%Ru/H-Beta and then 2.1 nm for 2%Ru/H-Beta. These observations agree well with the results from Ru dispersion analysis.

The ruthenium species on H-Beta support are investigated by H₂-TPR, as shown in Fig. 3. Since H-Beta is not reducible in the temperature range studied, the reduction peaks observed from 300 to 500 K should be due to the reduction of ruthenium species. For Ru/H-Beta with different ruthenium loadings, similar reduction peak centered at 423 K is observed and similar H₂/Ru ratio of ~2 is calculated from quantitative analysis. Obviously, ruthenium species should exist in the form of RuO₂ on H-Beta, which could be reduced to metallic ruthenium below 500 K. The temperature of RuO₂ reduction is similar to those observed for Ru/SiO₂ and Ru/SiO₂-Al₂O₃ [32], but slightly higher than unsupported RuO₂ due to the interaction between RuO₂ and support.

The acidic properties of Ru zeolites are evaluated by NH₃-TPD, as shown in Fig. 4. A broad ammonia desorption peak from 373 to 673 K is observed for Ru/Al₂O₃ while no distinct ammonia desorption is observed for Ru/SiO₂. For Ru supported on zeolites, two ammonia desorption peaks can be observed, i.e. a low-temperature peak at ~473 K and a high-temperature peak at over 573 K. According to the high-temperature desorption peak, the acidity of Ru catalysts is determined to be Ru/H-ZSM-5 (690 K) > Ru/H-Beta (610 K) > Ru/H-USY (600 K) > Ru/H-MOR (580 K).

3.2. Hydrodeoxygenation of diphenyl ether

The catalytic performance of bi-functional supported clusters was tested in the hydrodeoxygenation of diphenyl ether as a model reaction. As shown in Table 2, the catalytic activity and product selectivity are controlled by the catalysts employed. Typically, Rh/H-Beta shows the highest activity, followed by Ru/H-Beta and Pt/H-Beta, and then Pd/H-Beta with similar mole loading of metals. As for the product selectivity, higher selectivity toward desired product cyclohexane is achieved with Ru/H-Beta and Pt/H-Beta, followed by Rh/H-Beta and then Pd/H-Beta. Ruthenium appears to be the optimized noble metal considering its high activity and selectivity as well as its much lower price compared to others.

We investigated the effects of supports on the hydrodeoxygenation of diphenyl ether over Ru catalysts. As shown in Table 2, similar diphenyl ether conversion of ca. 70% is observed for all

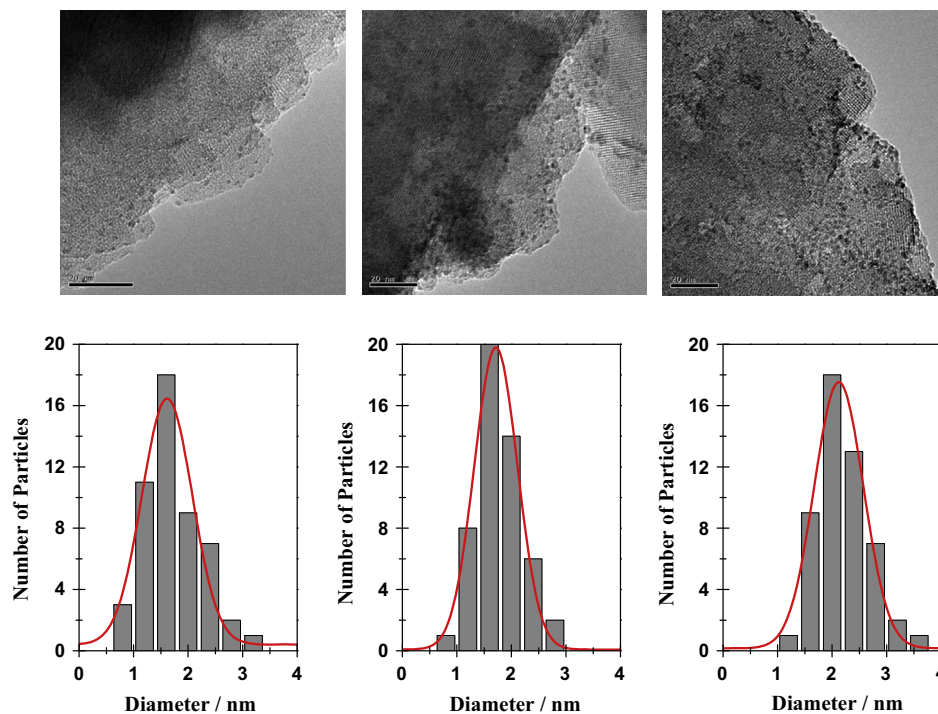


Fig. 2. TEM images and cluster size distribution of 0.5%Ru/H-Beta, 1%Ru/H-Beta and 2%Ru/H-Beta samples.

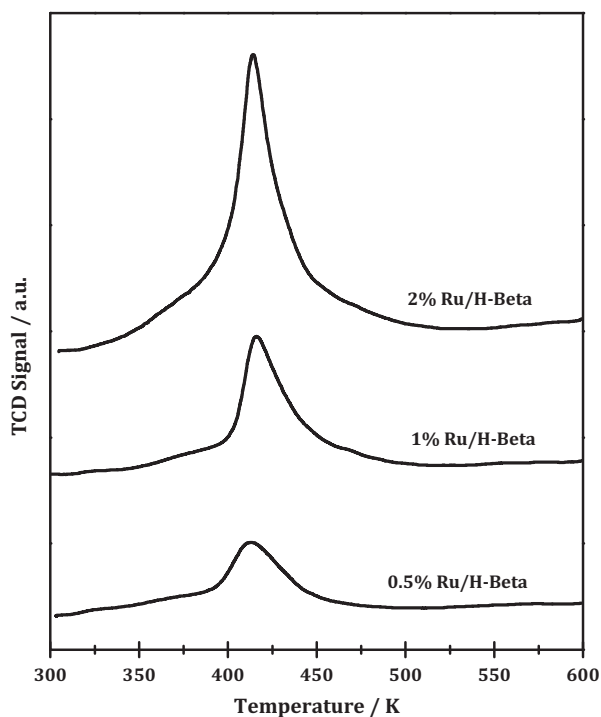


Fig. 3. H_2 -TPR profiles of 0.5%Ru/H-Beta, 1%Ru/H-Beta and 2%Ru/H-Beta samples.

supported Ru catalysts while the product distribution differs a lot. It seems that the acidity of supports can change the reaction pathway in hydrodeoxygenation process and, accordingly, influence the product distribution. Typically, the selectivity to desired product cyclohexane is observed to be Ru/H-ZSM-5 (73.2%) > Ru/H-Beta (66.0%) > Ru/H-USY (51.1%) > Ru/H-MOR (34.5%) > Ru/ Al_2O_3 (33.5%) > Ru/ SiO_2 (23.4%). For Ru supported on zeolites, the selec-

tivity to cyclohexane is relevant with the acidity of zeolite supports and higher selectivity is achieved with stronger acidity (Fig. 4). Besides, the product selectivity might also be influenced by the pore structure of zeolite. For Ru/H-ZSM-5, although highest cyclohexane selectivity is obtained, considerable amount of ether (11.1% dicyclohexyl ether and 13.2% cyclohexyl phenyl ether) is detected. This should be due to the fact that bulky ethers suffer from diffusion hindrance though the small channels of ZSM-5 zeolite (0.49 nm) and their further hydrodeoxygenation is therefore slow. This problem will become more evident for the hydrodeoxygenation of lignin-derived phenolic dimers over Ru/H-ZSM-5. Taking all the factors into consideration, Ru/H-Beta should be the optimized catalyst for the hydrodeoxygenation of lignin-derived compounds.

The effects of reaction temperature on the hydrodeoxygenation of diphenyl ether over 0.5%Ru/H-Beta catalyst are investigated, as shown in Table 3. Reaction temperature plays an essential role in the hydrodeoxygenation process. Typically, diphenyl ether conversion after 1 h reaction increases from 17.8% to 55.4% with increasing temperature from 373 to 413 K. Meanwhile, the selectivity to hydrocarbons, i.e. cyclohexane and benzene, dramatically increases from 35.5% to 96.2% (selectivity to cyclohexanol decreases from 48.2% to 3.2%). Obviously, the increasing reaction temperature can accelerate the conversion of cyclohexanol to cyclohexane. At temperature of 413 K and with bi-functional 0.5%Ru/H-Beta catalyst, the performance in hydrodeoxygenation of diphenyl ether is better or comparable with literature reports at much higher temperature, e.g. 473 K, and with other catalyst systems [3,13–27], demonstrating the great advantage of our catalyst system. Moreover, no Ru could be detected in the water phase after reaction, indicating no Ru leaching during reaction or the leached Ru below the detection limit.

The effects of ruthenium loadings on the of Ru/H-Beta catalyst are investigated and shown in Table 3. With ruthenium loading increases from 0.5% (0.049 mmol/g) to 1% (0.096 mmol/g), the diphenyl ether conversion increases from 55.4% to 80.5% (after reaction for 1 h). While diphenyl ether conversion decreases to

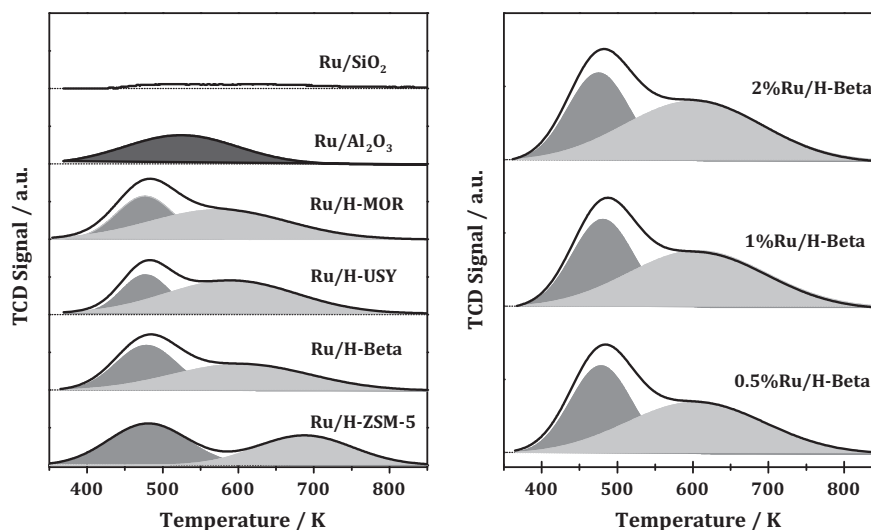
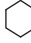
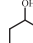
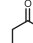
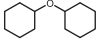
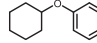


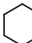
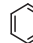
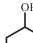
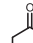
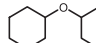
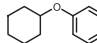
Fig. 4. NH_3 -TPD profiles of as-prepared supported Ru catalysts.

Table 2
Hydrodeoxygenation of diphenyl ether over different catalysts.^a

Catalyst	n_{Me} (mmol/g)	Conversion (%)	Selectivity (%)				
							
Rh/H-Beta	0.047	79.6	50.5	37.7	0.8	3.0	7.9
Pt/H-Beta	0.049	64.1	67.0	27.9	1.0	1.6	2.5
Pd/H-Beta	0.046	58.9	36.1	58.0	1.4	1.5	3.0
Ru/H-Beta	0.049	70.4	66.0	30.5	0	0.8	2.7
Ru/H-ZSM-5	0.050	74.5	73.2	2.5	0	11.1	13.2
Ru/H-USY	0.049	65.8	51.1	45.1	0.4	0.7	2.9
Ru/H-MOR	0.050	73.2	34.5	45.1	0	10.6	9.8
Ru/SiO ₂	0.049	72.0	23.4	51.2	0	12.6	12.9
Ru/Al ₂ O ₃	0.051	72.6	33.5	52.9	0	10.6	3.1

^a Reaction conditions: temperature = 393 K, time = 3 h.

Table 3
Hydrodeoxygenation of diphenyl ether over Ru/H-Beta catalyst.^a

Catalyst	Temp. (K)	n_{Ru} (mmol/g)	Conv. (%)	Selectivity (%)					
									
Ru/H-Beta	373	0.049	17.8	22.7	12.8	48.2	0	6.9	9.3
Ru/H-Beta	393	0.049	26.5	29.7	16.1	44.7	0	1.6	7.9
Ru/H-Beta	413	0.049	55.4	66.8	29.4	3.2	0.2	0.2	0.2
Ru/H-Beta	413	0.096	80.5	68.3	24.3	3.1	0.2	0.7	3.4
Ru/H-Beta	413	0.191	64.3	65.5	22.7	2.9	0.3	1.1	7.5

^a Reaction conditions: time = 1 h.

64.3% with ruthenium loading further increases to 2%. The TOF values are calculated to be 168.2, 136.8 and 66.7 h^{-1} for 0.5%Ru/H-Beta, 1%Ru/H-Beta and 2%Ru/H-Beta, respectively. Experimentally, 0.5% is the optimized ruthenium loading for Ru/H-Beta. The very low TOF value of 2%Ru/H-Beta seems to be strange and abnormal. Since the ruthenium cluster size (Fig. 2) and existence state (Fig. 3) are similar for Ru/H-Beta catalysts with different ruthenium loadings, they are not the decisive factors for the low TOF of the 2%Ru/H-Beta. The total density and strength of acid sites are also similar for Ru/H-Beta catalysts with different ruthenium loadings (Fig. 4), however, further experimental results reveal that the density of Lewis acid sites in Ru/H-Beta dramatically decreases with increasing Ru loading.

FTIR analysis with pyridine adsorption allows a clear distinction between Brønsted and Lewis acid sites. As a good Lewis base, pyridine molecules can interact with the Brønsted acid sites forming pyridinium ions (FTIR band at ca. 1540 cm^{-1}) and adsorb on the surface of Lewis acid sites through their isolated electron pair on nitrogen atoms (FTIR band at ca. 1450 cm^{-1}). As shown in Fig. 5, both Brønsted acid sites (60 $\mu\text{mol/g}$) and Lewis acid sites (112 $\mu\text{mol/g}$) can be identified for H-Beta support. The impregnation of ruthenium on H-Beta results in a distinct decline in the density of Lewis acid sites while the density of Brønsted acid sites is kept nearly unchanged. Typically, the density of Lewis acid sites decreases from 107 to 9 $\mu\text{mol/g}$ with increasing ruthenium loading from 0.5% to 2%. The synchronized decline in the Lewis acid site

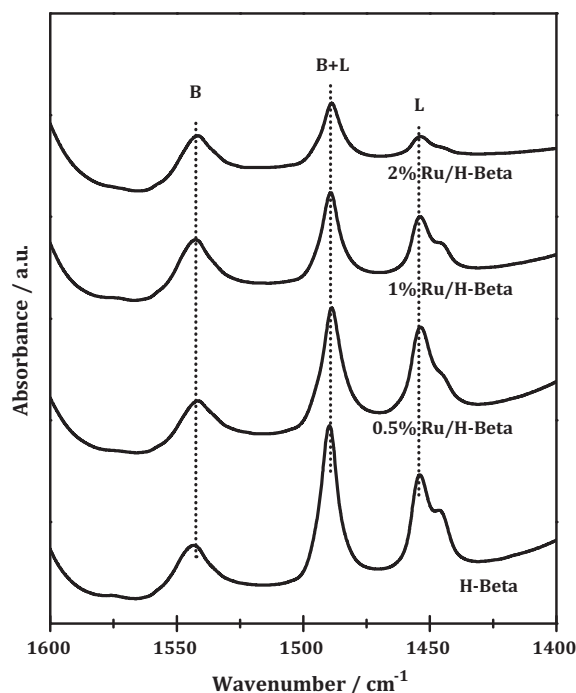


Fig. 5. FTIR spectra of H-Beta and Ru/H-Beta after pyridine adsorption and evacuation at 473 K. B: Brønsted acid sites; L: Lewis acid sites.

density and hydrodeoxygenation activity indicates the crucial role of Lewis acid sites in the hydrodeoxygenation of diphenyl ether over Ru/H-Beta catalyst.

3.3. Reaction pathway for the hydrodeoxygenation of diphenyl ether

The kinetic plots of diphenyl ether hydrodeoxygenation over 0.5%Ru/H-Beta catalyst at 413 K are shown in Fig. 6. Diphenyl ether conversion increases with reaction time and >95% conversion could be obtained after 3 h. At the early stage of hydrodeoxygenation reaction (reaction time of 0.5 h), benzene, cyclohexane and cyclohexanol are detected as major products while the selectivity to benzene is approximately equal to the sum of cyclohexane

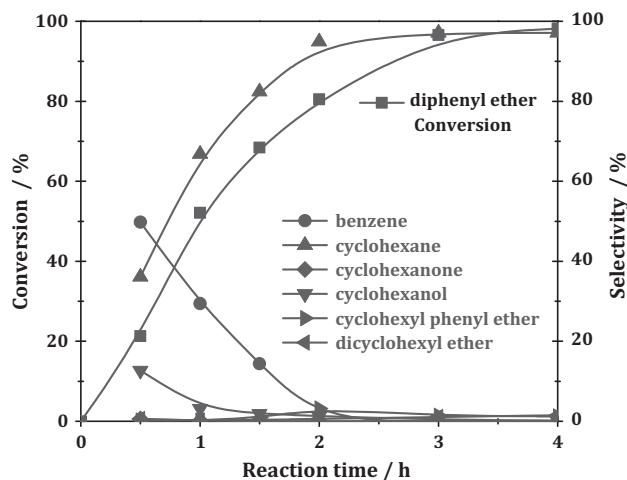


Fig. 6. Kinetic plots of diphenyl ether hydrodeoxygenation over 0.5%Ru/H-Beta catalyst. Reaction conditions: 2 mmol diphenyl ether, 4 mL H₂O, 0.2 g catalyst, 4 MPa H₂, temperature = 413 K.

and cyclohexanol. It is known that the hydrogenolysis of diphenyl ether produces equimolar benzene and phenol, which can be further converted to cyclohexane. The ca. 50% benzene selectivity at the early stage of hydrodeoxygenation reveals that the hydrogenolysis of diphenyl ether is much faster than the hydrogenation of benzene. The absence of phenol and cyclohexone indicates that the hydrogenation of phenol to cyclohexanol via cyclohexone as intermediate is a very fast reaction, with much higher rate than the dehydroxylation of cyclohexanol. With the extension of reaction time to 2 h, the benzene selectivity dramatically decreases to 0, while cyclohexane selectivity increases to >70%. During the reaction process, cyclohexyl phenyl ether and dicyclohexyl ether could be detected, indicating the existence of the direct hydrogenation of diphenyl ether. Since the selectivity to cyclohexyl phenyl ether and dicyclohexyl ether is rather low, the direct hydrogenation of diphenyl ether should be a minor pathway compared with hydrogenolysis. To verify the above assumption, the reaction rate of independent reaction step is measured and given in Table 4. It is seen that the hydrogenation of benzene catalyzed by Ru/H-Beta is very fast with TOF of 1168.2 h⁻¹. However, the presence of diphenyl ether can dramatically reduce the activity of Ru/H-Beta with a TOF of 125.6 h⁻¹ probably due to the blockage of ruthenium sites by hydroxyls and/or aromatic rings. On the basis of these observations, the reaction pathways of aqueous phase diphenyl ether hydrodeoxygenation over Ru/H-Beta are illustrated in Fig. 7. The major hydrodeoxygenation route is diphenyl ether hydrogenolysis into benzene and phenol. Benzene can be hydrogenated to cyclohexane on ruthenium and phenol hydrogenated to cyclohexanol via cyclohexone as intermediate. The formed cyclohexanol can be transformed to cyclohexane through a dehy-

Table 4

Rate of independent reaction step in the hydrodeoxygenation of diphenyl ether over 0.5%Ru/H-Beta.^a

Reaction step	TOF (h ⁻¹)
diphenyl ether → benzene + phenol → ...	171.3
benzene → cyclohexane	1168.2
benzene → cyclohexane ^b	125.6
phenol → cyclohexone → ...	1020.3
cyclohexone → cyclohexanol → ...	>2000
cyclohexanol → cyclohexane	151.1
cyclohexyl phenyl ether → dicyclohexyl ether → ...	127.0

^a Reaction conditions: 0.1 g 0.5%Ru/H-Beta, temperature = 413 K, time = 1 h.

^b In the presence of diphenyl ether.

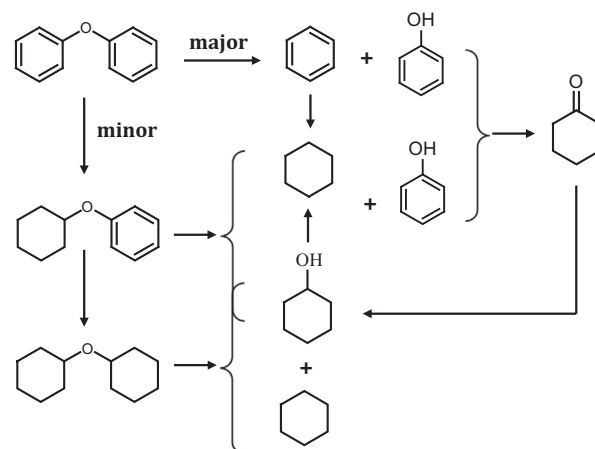


Fig. 7. Reaction pathways of diphenyl ether hydrodeoxygenation over 0.5%Ru/H-Beta.

droxyl step. The minor hydrodeoxygenation route is the direct hydrogenation of diphenyl ether to cyclohexyl phenyl ether and subsequent hydrogenation of cyclohexyl phenyl ether to dicyclohexyl ether. The hydrogenation products, i.e. cyclohexyl phenyl ether and dicyclohexyl ether, can undergo hydrogenolysis to cyclohexane, cyclohexanol and phenol. Furthermore, the stability of 0.5%Ru/H-Beta catalyst was evaluated via recycling experiments and no obvious decrease in diphenyl ether conversion could be observed within 5 cycles, indicating the good stability and recyclability of Ru/H-Beta catalyst.

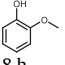
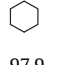
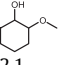
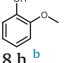
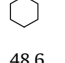
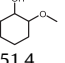
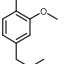
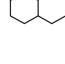
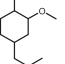
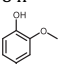
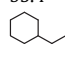
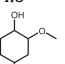
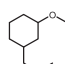
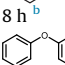
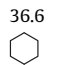
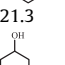
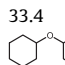
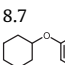
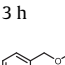
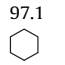
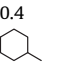
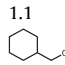
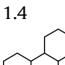
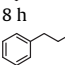
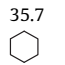
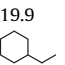
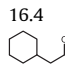
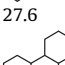
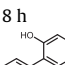
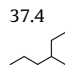
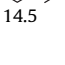
3.4. Hydrodeoxygenation of lignin-derived phenolic monomers/dimers

The hydrodeoxygenation of lignin-derived phenolic monomers and dimers is investigated with 0.5%Ru/H-Beta as optimized catalyst and the results are shown in Table 5. Two typical monomer products from the degradation of lignin, i.e. guaiacol and eugenol, can be efficiently converted into alkanes, with substrate conversion of >98% and selectivity to cycloalkanes of >95% obtained after 8 h. Meanwhile, some hydrogenation products could be observed (<5%). If 0.5%Ru/H-ZSM-5 is used as catalyst instead of Ru/H-Beta, high substrate conversion could also be obtained, however, considerable amount of by-product methoxycyclohexanols could be observed (Table 5). Similar results have been reported by Chen et al. in the hydrodeoxygenation of guaiacol catalyzed by Ru/H-ZSM-5 at 413 K for 4 h. It is therefore proposed that the Ru-catalyzed hydrogenation of aromatic ring is faster than the acid-catalyzed hydrolysis of the methoxy group [27]. The strength of acidity in Ru/H-ZSM-5 is distinctly higher than that in Ru/H-Beta (Fig. 4), however, Ru/H-Beta shows much higher activity for the hydrolysis of the methoxy group than Ru/H-ZSM-5. This should be due to the presence of Lewis acid sites in

Ru/H-Beta (Fig. 5), which greatly promotes the activation of C–O bond catalyzed by Lewis acid sites or the cooperation of Brønsted/Lewis acid sites.

β -O-4, α -O-4 and 4-O-5 linkages are three most common types of hardwood lignin [33] and therefore, we further investigated the hydrodeoxygenation of these representative lignin-derived phenolic dimers over 0.5%Ru/H-Beta. As shown in Table 5, the diphenyl ether (4-O-5) can be converted at 413 K with cyclohexane yield of >93%, which is comparable with other catalyst systems, e.g. Pd/C and H-ZSM-5 [15] and Ru/H-ZSM-5 [27], at much higher temperatures (473 K or above). For the hydrodeoxygenation of benzyl phenyl ether (α -O-4) and phenylethyl phenyl (β -O-4) over Ru/H-Beta, >99% substrate conversion could be obtained at 413 K after 8 h. In contrast to 4-O-5, the hydrodeoxygenation of α -O-4 and β -O-4 gives quite different product distributions. Typically, cyclohexane (35.7%), methyl cyclohexane (19.9%), cyclohexylmethanol (16.4%) and dicycloalkanes (27.6%) are detected as major products for the conversion of α -O-4 while cyclohexane (37.4%), ethylcyclohexane (24.0%), cyclohexylethanol (23.6%) and bicycloalkanes products (14.5%) for β -O-4. The relative high percentages of cyclohexylmethanol and cyclohexylethanol in the products should be due to their slow dehydroxylation rates (9.5 and 8.8 h⁻¹, respectively, in contrast to 1020.3 h⁻¹ for phenol). The product distribution of α -O-4 conversion is similar to that observed with ZSM-5 and Ni/ZSM-5 as catalysts at higher temperature of 523 K [34]. The product dicyclohexyl methane was proposed to be formed via free radical reaction that dominates the thermal pyrolysis process. The hydrodeoxygenation of mixed substrate, i.e. phenol/benzyl alcohol and phenol/toluene, over Ru/H-Beta was performed and the results are shown in Table 6. It is seen that single-ring products cyclohexane, methyl cyclohexane, cyclohexyl methanol are formed via hydrogenation and/or dehydroxylation, while only trace

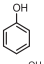
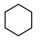
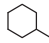
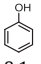
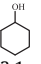
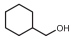
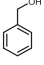
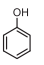
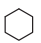
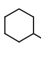
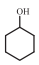
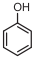
Table 5
Hydrodeoxygenation of lignin-derived phenolic monomers/dimers over 0.5%Ru/H-Beta.^a

Substrate	Conversion (%)	Selectivity (%)			Others
 8 h	98.8	 97.9	 2.1		
 8 h ^b	98.9	 48.6	 51.4		
 8 h	99.9	 95.4	 4.6		
 8 h ^b	99.8	 36.6	 21.3	 33.4	
 3 h	96.6	 97.1	 0.4	 1.1	 8.7
 8 h	99.0	 35.7	 19.9	 16.4	 1.4
 8 h	99.1	 37.4	 24.0	 23.6	 27.6
 8 h	99.9	 94.7		Ring-opening products 5.3	 14.5

^a Reaction condition: 2 mmol substrate, 0.2 g 0.5%Ru/H-Beta, 4 mL H₂O, temperature = 413 K;

^b With 0.5%Ru/H-ZSM-5 as catalyst.

Table 6
Hydrodeoxygenation of mixed substrate over 0.5%Ru/H-Beta.^a

Substrate	Conversion (%)	Product selectivity (%)					
		Single-ring		Double-ring			
	99.9						<0.2
	97.8	43.3	37.7	8.1	3.1	7.6	
	99.9						<0.1
	76.1	55.1		36.3		8.5	

^a Reaction condition: 1 + 1 mmol substrate, 0.1 g 0.5%Ru/H-Beta, 4 mL H₂O, temperature = 413 K, time = 1 h.

amount of double-ring products, e.g. dicyclohexyl methane, could be detected. That is, the thermal pyrolysis is the dominating route over hydrogenolysis and hydrolysis in the cleavage C–O–C linkages in α -O-4.

In addition to C–O–C, C–C linkage is another important aryl-aryl link type. The hydrodeoxygenation of 2,2-biphenol as 5–5' model compound is also investigated (Table 5). After reaction for 8 h, 99.9% conversion and 94.7% selectivity of desired product bicyclohexane are obtained. A small amount of ring-opening products are observed (5.3%), while no products from the cracking of C–C bond could be detected, excluding the cleavage the C–C linkage catalyzed by Ru/H-Beta under our reaction conditions.

4. Conclusions

In the present study, a bifunctional Ru/H-Beta catalyst system, namely highly dispersed RuO₂ nanoclusters of <2 nm on acidic zeolite H-Beta, was developed for bio-oil upgrading via the hydrodeoxygenation of lignin-derived phenolic compounds. Remarkable performance in the aqueous phase hydrodeoxygenation under very mild conditions, i.e. at 413 K and 4 MPa H₂, is achieved, which is ascribed to the optimized Ru active centers and the presence of both Brønsted and Lewis acid sites in zeolite support. Moreover, the reaction pathway is studied and the hydrogenolysis followed by hydrogenation and dehydroxylation is illustrated to be the dominant route.

Acknowledgements

This work is supported by the National Natural Science Foundation of China (21421001, 21373119), the Ministry of Education of China (IRT13022) and 111 Project (B12015).

References

- [1] Czernik S, Bridgwater AV. Overview of applications of biomass fast pyrolysis oil. *Energy Fuel* 2004;18:590–8.
- [2] Mohan D, Pittman CU, Steele PH. Pyrolysis of wood/biomass for bio-oil: a critical review. *Energy Fuel* 2006;20:848–89.
- [3] Yan N, Zhao C, Dyson PJ, Wang C, Liu L, Yuan K. Selective degradation of wood lignin over noble-metal catalysts in a two-step process. *ChemSusChem* 2008;1:626–9.
- [4] Song Q, Wang F, Cai J, Wang Y, Hang J, Yu W, Xu J. Lignin depolymerization (LDP) in alcohol over nickel based catalysts via a fragmentation-hydrogenolysis process. *Energy Environ Sci* 2013;6:994–1007.
- [5] Jiang Z, He T, Li J, Hu C. Selective conversion of lignin in corn cob residue to monophenols with high yield and selectivity. *Green Chem* 2014;16:4257–65.
- [6] Garcia-perez M, Chaala A, Pakdel H, Kretschmer D, Roy C. Characterization of bio-oils in chemical families. *Biomass Bioenergy* 2007;31:222.
- [7] Zhao C, Lercher JA. Upgrading pyrolysis oil over Ni/HZSM-5 by cascade reactions. *Angew Chem Int Ed* 2012;51:5935–40.
- [8] Zhang X, Zhang Q, Wang T, Ma L, Yu Y, Chen L. Hydrodeoxygenation of lignin-derived phenolic compounds to hydrocarbons over Ni/SiO₂–ZrO₂ catalysts. *Bioresour Technol* 2013;134:73–80.
- [9] Yoosuk B, Tumnantong D, Prasassarakich P. Amorphous unsupported Ni–Mo sulfide prepared by one step hydrothermal method for phenol hydrodeoxygenation. *Fuel* 2012;91:246–52.
- [10] Li K, Wang R, Chen J. Hydrodeoxygenation of anisole over silica-supported Ni₂P, MoP, and NiMoP catalysts. *Energy Fuel* 2011;25:854–63.
- [11] Echeandia S, Arias PL, Barrio VL, Pawelec B, Fierro JLG. Synergy effect in the HDO of phenol over Ni–W catalysts supported on active carbon: Effect of tungsten precursors. *Appl Catal B* 2010;101:1–12.
- [12] Wang C, Wang D, Wu Z, Wang Z, Tang C, Zhou P. Effect of W addition on the hydrodeoxygenation of 4-methylphenol over unsupported NiMo sulfide catalysts. *Appl Catal A* 2014;476:61–7.
- [13] Zhao C, Kou Y, Lemonidou AA, Li X, Lercher JA. Highly selective catalytic conversion of phenolic bio-oil to alkanes. *Angew Chem Int Ed* 2009;48:3987–90.
- [14] Zhao C, He J, Lemonidou AA, Li X, Lercher JA. Aqueous-phase hydrodeoxygenation of bio-derived phenols to cycloalkanes. *J Catal* 2011;280:8–16.
- [15] Zhao C, Lercher JA. Selective hydrodeoxygenation of lignin-derived phenolic monomers and dimers to cycloalkanes on Pd/C and HZSM-5 catalysts. *ChemCatChem* 2012;4:64–8.
- [16] Zhao C, Song W, Lercher JA. Aqueous phase hydroalkylation and hydrodeoxygenation of phenol by dual functional catalysts comprised of Pd/C and H/La-BEA. *ACS Catal* 2012;2:2714–23.
- [17] Zhu X, Lobban L, Mallinson R, Resasco D. Bifunctional transalkylation and hydrodeoxygenation of anisole over a Pt/HBeta catalyst. *J Catal* 2011;281:21–9.
- [18] Xu W, Miller SJ, Agrawal PK, Jones CW. Depolymerization and hydrodeoxygenation of switchgrass lignin with formic acid. *ChemSusChem* 2012;5:667–75.
- [19] Nimmanwudipong T, Aydin C, Lu J, Runnebaum RC, Brodwater LC, Browning ND, Block DE, Gates BC. Upgrading of lignin-derived compounds: reactions of eugenol catalyzed by HY zeolite and by Pt/ γ -Al₂O₃. *Catal Lett* 2012;142:151–60.
- [20] Lin Y, Li C, Wan H, Lee H, Liu C. Catalytic hydrodeoxygenation of Guaiacol on Rh-based and sulfided CoMo and NiMo catalysts. *Energy Fuel* 2011;25:890–6.
- [21] Wildschut J, Melián-Cabrera I, Heeres HJ. Catalyst studies on the hydrotreatment of fast pyrolysis oil. *Appl Catal B* 2010;99:298–306.
- [22] Newman C, Zhou X, Goundie B, Ghampton IT, Pollock RA, Ross Z, et al. Effects of support identity and metal dispersion in supported ruthenium hydrodeoxygenation catalysts. *Appl Catal A* 2014;477:64–74.
- [23] Yan N, Yuan Y, Dykeman R, Kou Y, Dyson PJ. Hydrodeoxygenation of lignin-derived phenols into alkanes by using nanoparticle catalysts combined with Brønsted acidic ionic liquids. *Angew Chem Int Ed* 2010;49:5549–53.
- [24] Xu H, Wang K, Zhang H, Hao L, Xu J, Liu Z. Ionic liquid modified montmorillonite-supported Ru nanoparticles: highly efficient heterogeneous catalysts for the hydrodeoxygenation of phenolic compounds to cycloalkanes. *Catal. Sci. Technol.* 2014;4:2658–63.
- [25] He J, Zhao C, Lercher JA. Impact of solvent for individual steps of phenol hydrodeoxygenation with Pd/C and HZSM-5 as catalysts. *J Catal* 2014;309:362–75.
- [26] Hong D-Y, Miller SJ, Agrawal PK, Jones CW. Hydrodeoxygenation and coupling of aqueous phenolics over bifunctional zeolite-supported metal catalysts. *Chem Commun* 2010;46:1038–40.
- [27] Wei Z, Chen J, Liu R, Wang S, Chen L, Li K. Hydrodeoxygenation of lignin-derived phenolic monomers and dimers to alkane fuels over bifunctional zeolite-supported metal catalysts. *ACS Sustain. Chem. Eng.* 2014;2:683–91.
- [28] Zhang J, Teo J, Chen X, Asakura H, Tanaka T, Teramura K, Yan N. A series of NiM (M = Ru, Rh, and Pd) bimetallic catalysts for effective lignin hydrogenolysis in water. *ACS Catal.* 2014;4:1574–83.

- [29] Zhang J, Asakura H, van Rijn J, Yang J, Duchesne P, Zhang B, Chen X, Zhang P, Saeys M, Yan N. Highly efficient, NiAu-catalyzed hydrogenolysis of lignin into phenolic chemicals. *Green Chem* 2014;16:2432–7.
- [30] Chen X, Yan N. Novel catalytic systems to convert chitin and lignin into valuable chemicals. *Catal. Surveys Asia* 2014;18:164–76.
- [31] Emeis CA. Determination of integrated molar extinction coefficients for Infrared absorption bands of pyridine adsorbed on solid acid catalysts. *J Catal* 1993;141:347–54.
- [32] Chen L, Li Y, Zhang X, Zhang Q, Wang T, Ma L. Mechanistic insights into the effects of support on the reaction pathway for aqueous-phase hydrogenation of carboxylic acid over the supported Ru catalysts. *Appl Catal A* 2014;478:117–28.
- [33] Zakzeski J, Bruijninckx PCA, Jongerius AL, Weckhuysen BM. The catalytic valorization of lignin for the production of renewable chemicals. *Chem Rev* 2010;110:3552–99.
- [34] He J, Lu L, Zhao C, Mei D, Lercher JA. Mechanisms of catalytic cleavage of benzyl phenyl ether in aqueous and apolar phases. *J Catal* 2014;311:41–51.